

Supplementary Document

Circularly Polarized High-Gain Fabry-Perot Cavity Antenna with High Sidelobe Suppression

1. The results of the feeder

The reflection coefficient and 3D radiation pattern of the feeder are shown in Figures S1 and S2, respectively.

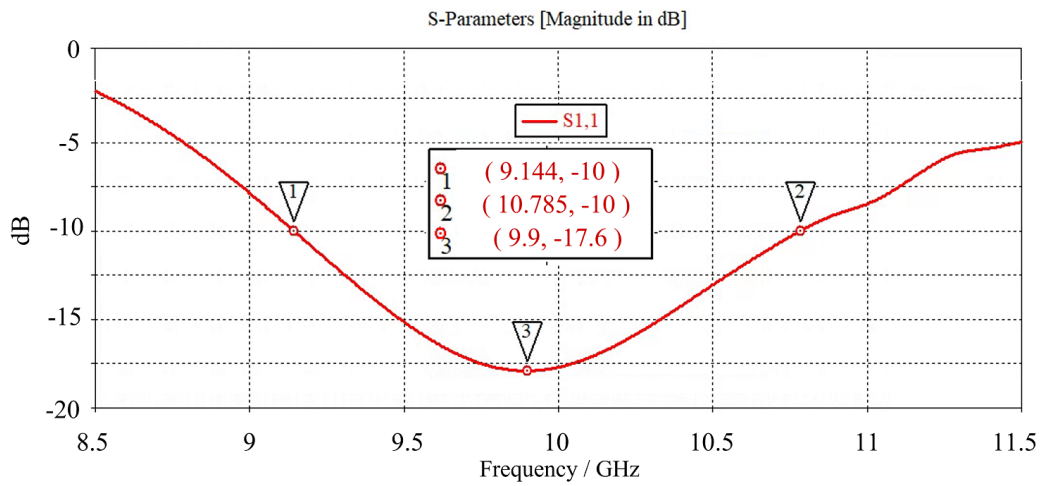


Figure S1. The reflection coefficient of the MPA.

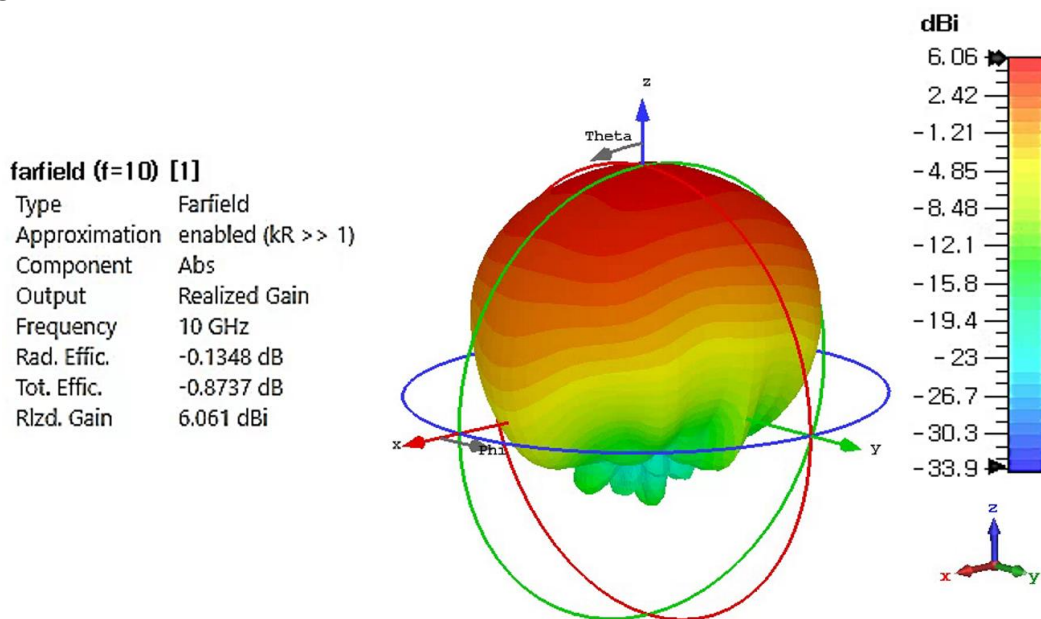
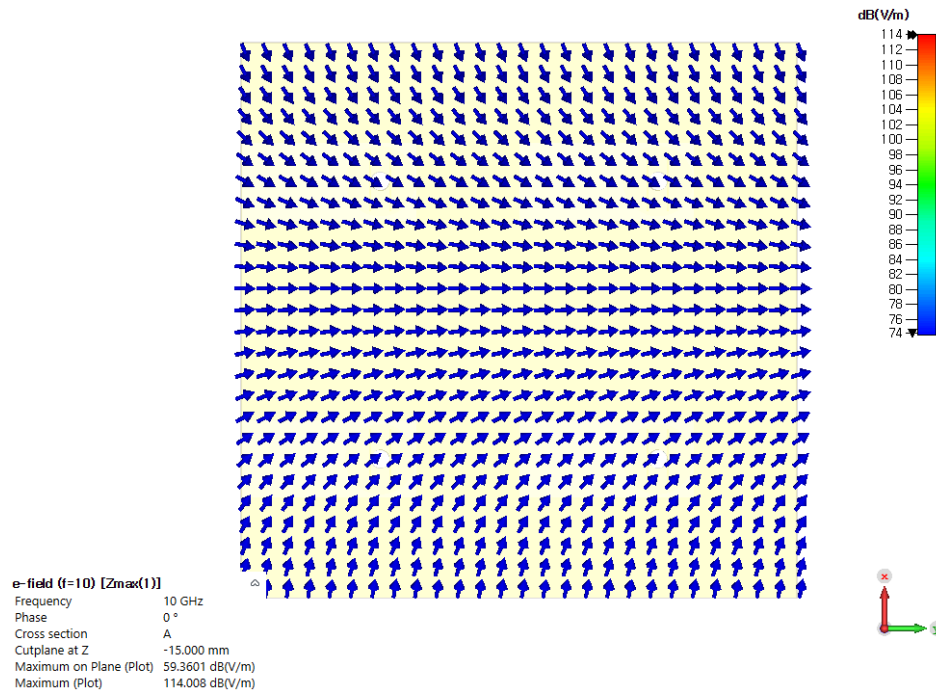


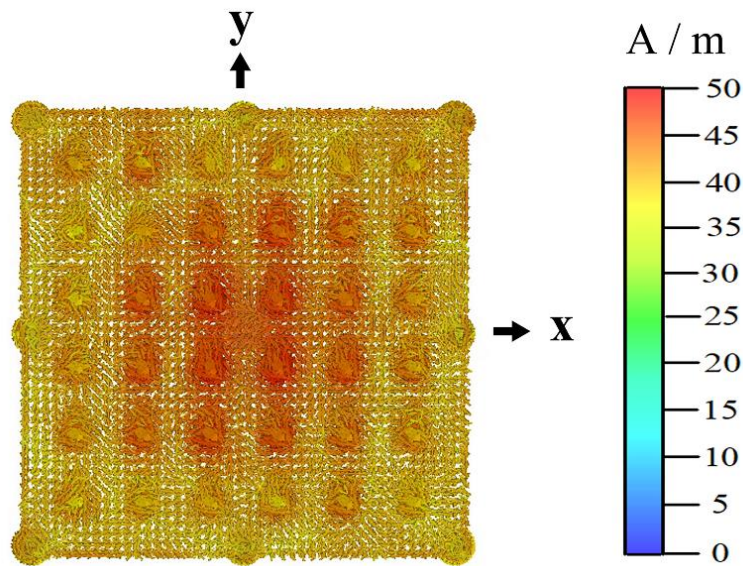
Figure S2. The 3D radiation pattern of the MPA.

2. The E_x -field distribution above the PRS unit cell and surface current density above the CP-PRS superstrate

The E_x -field distribution is illustrated at 15 mm above the PRS unit cell to confirm the circular polarization in the broadside direction in Figure S3(a). Moreover, the surface current density above the CP-PRS superstrate is also shown in Figure S3(b).



(a)



(b)

Figure S3. (a) The E_x -field distribution at 15 mm above the PRS unit cell, (b) the surface current density above the CP-PRS superstrate.

3. The results of the circularly polarized FPCA

The impedance measurement of the CP-FPCA

The impedance measurement of the CP-FPCA respecting cavity height is depicted in Figure S4, which is performed on a 40 GHz vector network analyzer (Anritsu VNA; MS46122A) using the short-open-load (SOL) – Anritsu calibration kit; TOSLKF50A-40, type K(f), 50 Ω – standardized calibration approach.

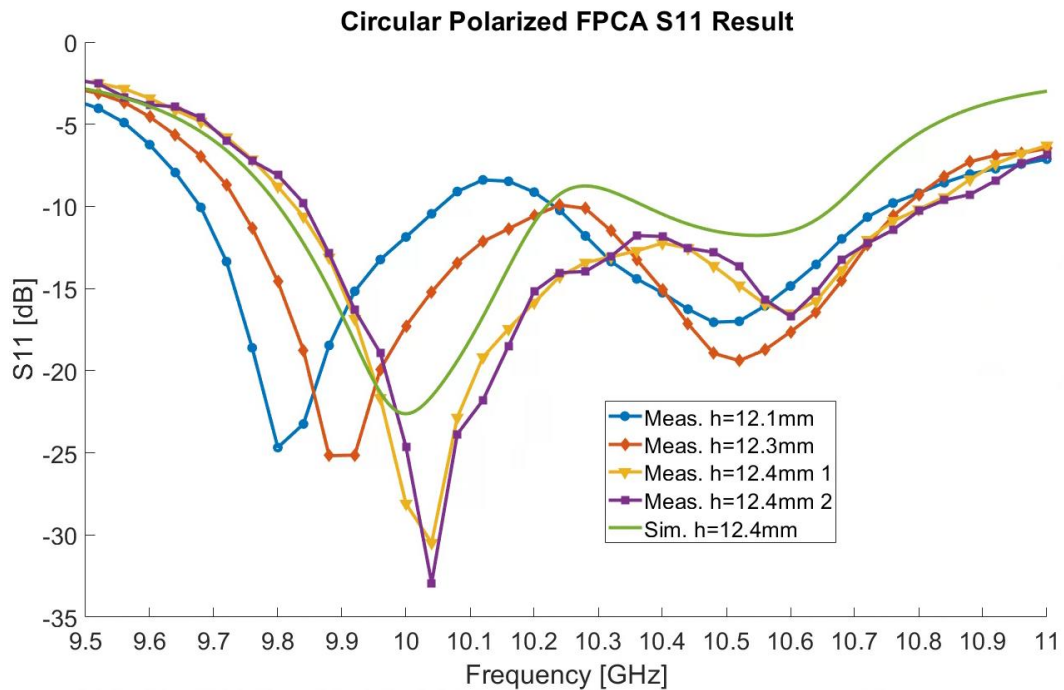


Figure S4. The impedance measurement of the CP-FPCA.

The 3D radiation pattern of the CP-FPCA

The 3D radiation pattern of the CP-FPCA is illustrated in Figure S5.

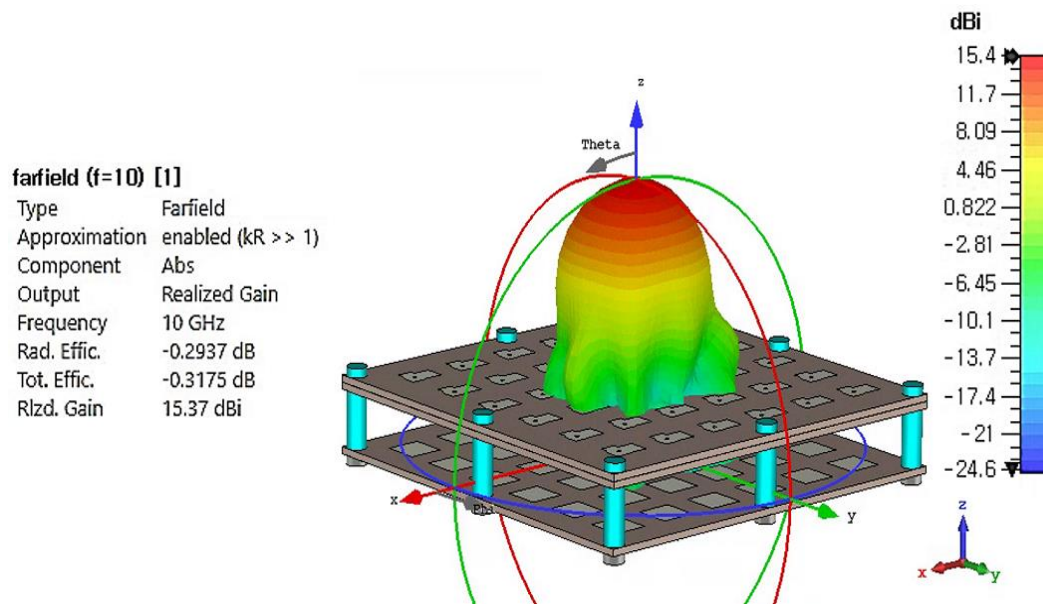
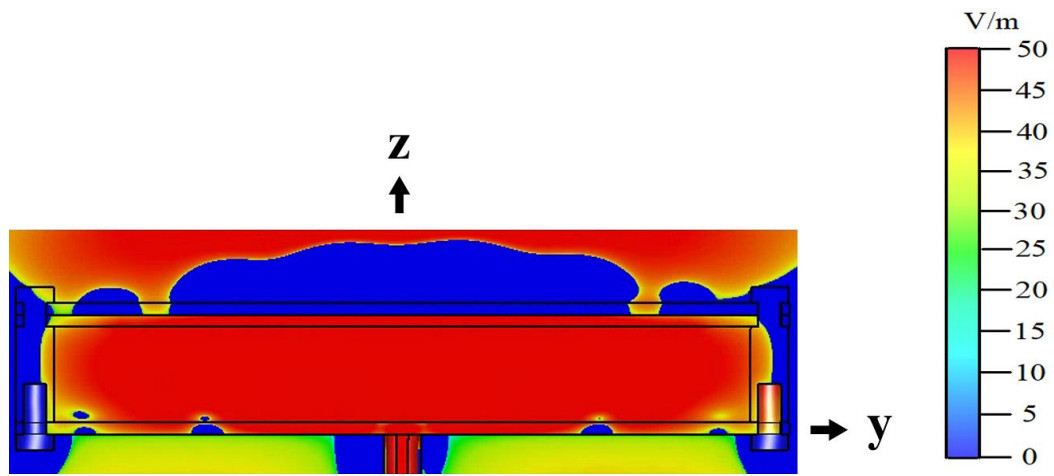


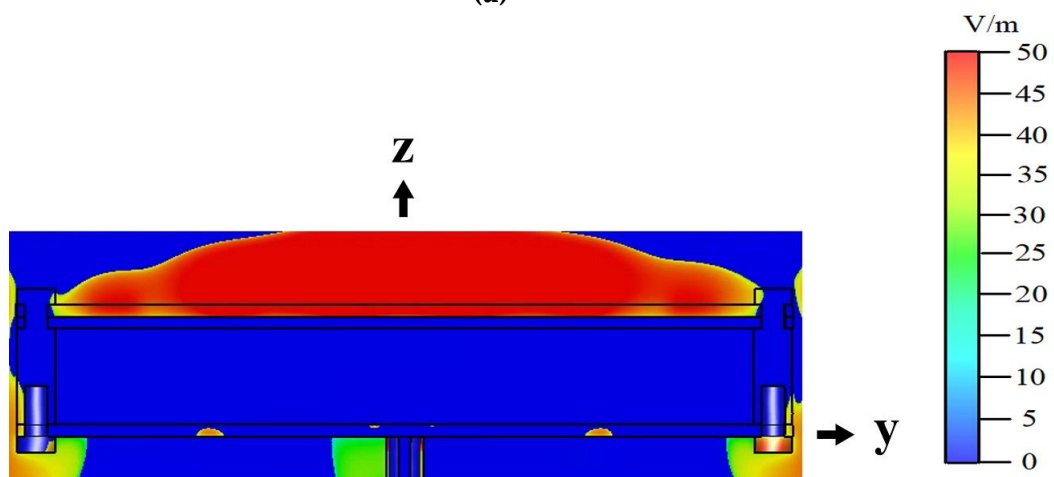
Figure S5. The 3D radiation pattern of the CP-FPCA.

Ex-field distribution within and above the resonance cavity

The *Ex*-field distribution within the CP-FPCA is depicted in Figure S6(a) to confirm the constructive interference, which satisfies Trentini's beamforming condition. In Figure S6(b), the *Ex*-field above the CP-FPCA is illustrated.



(a)



(b)

Figure S6. The E_x -field distribution (a) within the CP-FPCA, (b) above the CP-FPCA.